Palaeogeography, Palaeoclimatology, Palaeoecology 445 (2016) 72–82

Contents lists available at ScienceDirect

Palaeogeography, Palaeoclimatology, Palaeoecology

journal homepage: www.elsevier.com/locate/palaeo

Mineral and elemental indicators of post-glacial changes in sediment delivery and deposition under a western boundary upwelling system (Cabo Frio, southeastern Brazil)

Ana Luiza Albuquerque [a], Philip Meyers [b,*], Andre L. Belem [d], Bruno Turcq [c], Abdelfettah Siffedine [c,e], Ursula Mendoza [a], Ramsés Capilla [f]

[a] Departamento de Geoquímica, Universidade Federal Fluminense, 24020-150 Niterói, RJ,Brazil
[b] Department of Earth and Environmental Sciences, The University of Michigan, Ann Arbor, MI 48109-1005, USA
[c] Institut de Recherche pour le Développement, France (IRD), LOCEAN, UMR 7159 CNRS-IRD-Univ P. et M. Curie-MNHN, 32, Avenue Henri Varagnat, 93143 Bondy cedex, France
[d] Departamento de Engenharia Agricola e Ambiental, Universidade Federal Fluminense, Niterói, Brazil
[e] LMI PALEOTRACES (Institut de Recherche pour le Développement—France, Universidade Federal Fluminense—Brazil, Universidad de Antofagasta-Chile) Departamento de Geoquímica, 24202-150 Niterói, Brazil
[f] Petrobras–Cenpes, Cidade Universitária, Ilha do Fundão, RJ 21941-915, Brazil

ARTICLE INFO

Article history:
Received 9 June 2015
Received in revised form 14 December 2015
Accepted 5 January 2016
Available online 13 January 2016

Keywords:
Clay minerals
Trace elements
Southeastern Brazilian continental shelf
Mass accumulation rates
Postglacial sea level changes

ABSTRACT

Minerals and elements are important proxies that can provide information about variations in the delivery and deposition of coastal ocean sediments associated with past climate changes. In this study, postglacial changes in the accumulation of sediments on the upper shelf of southeastern Brazil are linked to the evolution of regional paleoceanographic and continental paleoclimatic conditions during the last 14.4 kyr CAL BP. Mineralogical and major and trace element analyses of a ^{14}C-dated sediment core identify three main lithostratigraphic units of this core that reveal a succession of changes in sediment delivery and accumulation as postglacial sea level rose and Holocene climate on land evolved. The depositional setting has transitioned in response to the large sea level rise prior to 9.9 kyr CAL BP from being a shallow water high energy environment to a deeper water one. This location has since then been a lower energy environment that has persisted into modern times. Due to the high marine productivity associated with the Cabo Frio upwelling system in an oxygenated water column, the sediments have shown a complex and dynamic redox condition, making variations in redox-sensitive trace elements indicative of changes in primary production and organic matter diagenesis at this location. After sea level stabilized ~9 kyr CAL BP, variations in fluxes of Al, Fe, Ca, and minerals were small, indicating that climate driven changes had only secondary controls on delivery of detrital sediment components to the Cabo Frio shelf. Modern coastal upwelling conditions and the onset of mid-shelf organic-rich sediment deposition were established after 9.9 CAL kyr BP.

1. Introduction

Accumulations of sediment in near shore areas of the ocean are sensitive to a variety of processes. Changes in marine productivity, delivery of continental components, coastal currents, and ocean dynamics are some of the factors that can affect the deposition and composition of sediments over time (Meyers, 1997). In addition, postglacial sea level rise has had a profound long-term effect on shelf sediments because of its impacts on many of these factors. The Southeastern Brazilian Shelf off Cabo Frio hosts a western boundary upwelling system that makes it a particularly suitable area to study the interplay of these multiple processes (e.g., Mahiques et al., 2011; Mendoza et al., 2014). The combination of classic coastal upwelling, mid-shelf wind curl, and shelf-margin meanders of the Brazil Current (BC) stimulates inner shelf upwelling and mid-shelf intrusion of nutrient-rich waters into the euphotic zone, thereby producing high rates of marine productivity (Belem et al., 2013; Albuquerque et al., 2014). In addition, the regional complexity of oceanographic circulation driven by boundary current interactions with the shelf provides a wide spectrum of sediment distribution patterns (Mendoza et al., 2014). The coast around Cabo Frio also features small and medium size rivers that may have delivered important amounts of continental sediments to the coastal region during the Last Glacial Maximum. Subsequent progressive sea-level rise generally diminished distribution of this terrigenous material to the outer shelf and slope (Mendoza et al., 2014). More recently, the

* Corresponding author at: Department of Earth and Environmental Sciences, The University of Michigan, 1100 North University Avenue, Ann Arbor, Michigan 48109-1005, USA. Tel.: +1 734 764 0597; fax: +1 734 763 4690.
E-mail address: pameyers@umich.edu (P. Meyers).

http://dx.doi.org/10.1016/j.palaeo.2016.01.006
0031-0182/

shelf has experienced an increase of terrigenous input during the last 5 kyr CAL BP (Mahiques et al., 2002) that probably reflects changes in the river catchments and that has repositioned locations of fluvial sediment delivery and deposition.

Bulk mineral assemblages provide several types of proxies that can be used to investigate some of these potential postglacial changes in sediment delivery and deposition. Indeed, sea level variations and their effects on the physiography of coastal areas can be reflected in changes in the fluvial sources and in the biogenic or lithogenic mineral assemblages (Diester-Haass et al., 2002). The biogenic sediment components include the opal particulate remains of radiolarians (Pisias et al., 2007) and diatoms (Barron and Bukry, 2007) that are especially predominant in upwelling areas. Preservation of the amorphous biogenic silica in marine sediments can be ten times higher than organic carbon (Treguer et al., 1995), showing its greater potential as a paleoproductivity proxy. Carbonate components are contributed to marine sediments by foraminifera, coccolithophores, ostracodes, and bivalves. Grain-size distributions of both biogenic and lithogenic components are related to regional and local hydrodynamics as well as the dominance of different minerals. For example, sediments deposited in high energy hydrodynamic settings have elevated contents of quartz-rich sands, whereas those deposited in low energy environments typically consist of muddy sediments rich in illite and kaolinite and have a higher potential for organic matter preservation (Keil and Hedges, 1993) that can influence authigenic sedimentary processes.

Trace element compositions can provide especially important information about postglacial changes in sedimentation. Changes in marine productivity and their possible effects on bottom-water chemistry are often be recorded by productivity- and redox-sensitive trace elements (e.g., Calvert and Pedersen, 1993; Tribovillard et al., 2006). For example, the relation found between the abundance of biogenic barite ($BaSO_4$) and organic matter and the refractory nature of barite in sediments where intense sulfate reduction does not take place make biogenic barium a good proxy for paleoproductivity (e.g., Dymond et al., 1992; François et al., 1995). In some cases, large fluxes of oxidizable organic matter to the sea floor can deplete dissolved oxygen faster than oceanic ventilation can replace it, leading to anoxygenic reducing conditions that destabilize barite. Under these conditions, some trace elements (e.g., Cd, Cu, Mo, Zn) can accumulate under the consequent anoxic/sulfidic conditions because they coprecipitate with pyrite or form insoluble sulfides (cf., Calvert and Pedersen, 1993). The valence states of other trace elements (e.g., Cr, Mo, Re, U, V) are redox-sensitive, causing these elements to accumulate under suboxic/anoxic conditions due to their reduction to less soluble forms at the redox-boundary (e.g., Crusius et al., 1996; Warning and Brumsack, 2000; Brumsack, 2006). In contrast, trace elements such as Fe and Mn become soluble under low oxygen conditions in sediments and can migrate within sediment pore water. In addition, less reactive trace elements can serve as important indicators of the source and supply of land-derived sediments to the sea floor. For example, Arz et al. (1998) described variations in Ca, Ti, and Fe in a well-oxygenated sediment sequence that was deposited over the past 85 kyr off the coast of northeastern Brazil that reflect past climate-related pulses in the delivery of continental sediments. Finally, changes in the mass accumulation rates (or fluxes) of trace element components can reflect changes in the rates of fluvial delivery of these sedimentary materials to inner shelf areas (Swarzenski et al., 2006).

The glacial melting that accompanied the termination of the Last Glacial Maximum caused prodigious amounts of fresh water to be added to the North Atlantic Ocean. The massive inputs of cold, fresh water may well have altered the density-driven thermohaline circulation patterns of the ocean, and they often coincided with indications of millennial scale global climate fluctuations. Some of these climate oscillations, such as the Heinrich Event H0 (~12 ka; Hemming, 2004), Bond events B8 to B1 (11.1–1.4 ka; Bond et al., 1997) and the Younger Dryas (12.8–11.5 ka; Muscheler et al., 2008), have potentially left some imprints in the Southeastern Brazilian Shelf sediment record. It is known that Heinrich events provoked southern displacement of the Intertropical Convergence Zone (ITCZ, Leduc et al., 2007), which could influence geostrophic oceanic circulation and wind patterns in the Cabo Frio region from the repositioning of the South Atlantic High (SAH). Souto et al. (2011) showed that the availability of the South Atlantic Central Water (SACW) on the shelf of the Cabo Frio region during the last 1.2 kyrs responded to displacements of the ITCZ and the SAH during the Medieval Climate Anomaly (MCA) and the Little Ice Age (LIA). In addition, abrupt changes in the South American Monsoon System (SAMS) during the Holocene have affected regional precipitation (e.g., Stríkis et al., 2011; Vuille et al., 2012) and thereby created changes in fluvial delivery of water and eroded sediments to the Southeastern Brazilian Shelf.

As part of our investigation of the Holocene paleoceanographic and paleoclimatic history of the Southeastern Brazilian Shelf upwelling system, we have studied a sediment core that provides a record of coastal sediment accumulation over the past 14.4 kyr. During this interval of postglacial time, global sea level has risen by approximately 100 m (Bard et al., 1996; Guilderson et al., 2000; Tarasov and Peltier, 2005), and the climate of southeastern Brazil has experienced several fluctuations in the amount of precipitation it receives (Rodrigues-Filho et al., 2002) and consequently in its continental drainage. Consequences of the sea level rise are shifts in the positions of the shorelines and of the upwelling associated high productivity relative to the coring location near Cabo Frio. The changes in precipitation are likely to have caused changes in the amounts of erosion and delivery of land-derived sediments to this near shore area. To explore these possibilities, we used the bulk mineral and trace element compositions and fluxes as proxies of the changes in sedimentation. We describe changes in the elements as indicators for changes in the delivery and deposition of sediments on the midshelf, and we discuss these variations in sediment composition and consider the changes in oceanic and continental conditions that they imply.

2. Regional setting

2.1. Southeastern Brazilian Shelf

The sediment coring location is on the middle of the Southeastern Brazilian Shelf off Cabo Frio (Fig. 1), which is a position that marks the boundary of the two distinct oceanographic provinces of the Campos and Santos basins (Cainelli and Webster, 1999). Cabo Frio also delineates an abrupt change in the orientation of the coastline from NE–SW in the Campos Basin to E–W in the Santos Basin that is accompanied by the orientation of the shelf edge (Campos et al., 2000). The E–W coast is exposed to SW–SE winds associated with cold fronts, whereas the NE–SW portion is typically exposed to NE-E winds that drive coastal upwelling. The continental shelf north of Cabo Frio is characterized by a complex bathymetry (Fainstein and Summerhayes, 1982), in contrast with the South Brazil Bight (Santos Basin), which has a crescent shape and is generally bathymetrically smooth.

The water mass structure over the shelf is a result of mixing of three water masses: the oligotrophic warm and salty Tropical Water (TW; $T > 20$ °C; $S > 36.40$), carried by the BC; the colder and nutrient-rich SACW ($T < 20$ °C; $S > 36.40$; Castro and Miranda, 1998), which is also transported by the BC and is associated with the upper part of the permanent thermocline; and the Coastal Water (CW), a low-salinity, warmer water body resulting from coastal processes (plumes) and continental fresh water inputs. Because the contribution of fresh water from river discharges is negligible, some studies define the low salinity water on the shelf as the Subtropical Shelf Water (SSW) (Piola et al., 2000; Venancio et al., 2014).

The Campos Basin receives freshwater inputs from small to medium size rivers that are located approximately 150 km north of Cabo Frio, primarily the Paraíba do Sul River that has a discharge ranging from

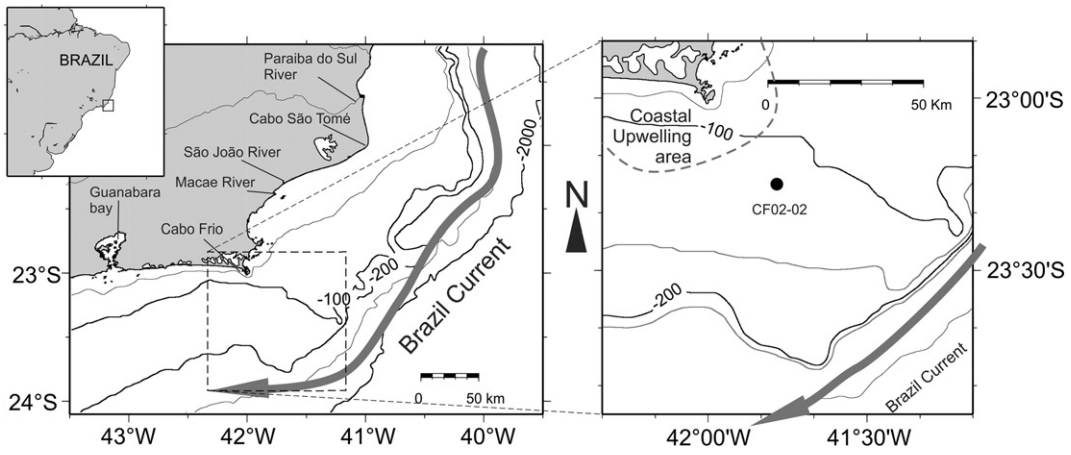

Fig. 1. Location of Core CF02-02B offshore of Cabo Frio and the locations of the main small and medium size rivers and of Guanabara Bay that provide land-derived sediments to the shelf. Regional bathymetry in meters and the location of local upwelling zones are shown. The inset displays the location of Cabo Frio relative to southeastern Brazil. Representative position of the main flow of the Brazil Current flux as summarized by Silveira et al. (2000) is also shown.

4400 to 180 $m^3 \cdot s^{-1}$ (Carvalho et al., 2002) and sediment yield of 25–30 $t \cdot km^{-2} \cdot yr^{-1}$ (Jennerjahn et al., 2010), as well as the small Sao Joao and Macae rivers. Although there are no large rivers in the South Brazil Bight, freshwater inputs can occur from several estuaries that generally function as sediment "trap-and-go" features to the inner shelf. In particular, dispersion of the Guanabara Bay plume can occasionally reach the Cabo Frio shelf and contribute both dissolved and particulate matter (Albuquerque et al., 2014).These contributions to the dissolved and particulate phases of continental material, in combination with the coastal Ekman transport and eddy-induced activity in the mid-shelf, can lead to a complex mixture of signals from different sources and can affect the composition of biogenic elements and the governing biogeochemical cycles as a whole. In addition, the contribution of terrestrial organic material to the Cabo Frio shelf has been confirmed by Yoshinaga et al. (2008), Oliveira et al. (2013) based on the presence of plant-wax lipids in the sediments, as well as by Albuquerque et al. (2014) from moored-sediment trap collections on the shelf border.

As discussed by Mahiques et al. (2002, 2004), Mendoza et al. (2014), sediment transport on the Cabo Frio inner shelf is controlled by wind-driven circulation and by coastal current remobilization and transport, whereas sediment transport on the outer shelf is dominated by the meandering of the internal front of the BC. In contrast, mid-shelf sediment transport is primarily modulated by the wind curl (Castelao and Barth, 2006), augmented by contributions from cross-shelf upwelled coastal waters (Belem et al., 2013). Continental sediment supply for the Cabo Frio shelf is probably provided by different sources with variable magnitudes, such as small and medium size local rivers, the Paraiba do Sul River north of Cabo Frio, and Guanabara Bay west of Cabo Frio (Albuquerque et al., 2014; Mendoza et al., 2014).

2.2. Brazil current and the western boundary upwelling system

Circulation on the Southeastern Brazilian Shelf is mainly controlled by the BC, which flows southward following the 200 m isobath and transports TW from the tropical South Atlantic in its upper levels and SACW between 200 and 700 m (Campos et al., 2000). This typical Western Boundary Current is highly influenced by the Subtropical Gyre and the SAH (Peterson and Stramma, 1991), which imparts the common oligotrophic character to western boundary continental shelves and carries salty and warmer tropical waters poleward. However, the BC interacts with the coastal system to promote a subsurface upwelling of SACW on the shelf edge and a shelf intrusion through current encroachment (Roughan and Middleton, 2002; Aguiar et al., 2014). Northeasterly winds that favor upwelling predominate during the spring and summer for periods of many days and are associated with surface cold-water events near the Cabo Frio coast (Franchito et al., 2008). The temperature contrast between cold coastal upwelling waters and the inner front of the warmer BC on the shelf border promotes a negative wind stress curl that generates an ocean surface divergence, resulting in upward Ekman pumping in the mid shelf (Castelao and Barth, 2006; Castelao, 2012). The subsurface presence of SACW on the shelf enriches the water column with nutrients, significantly affecting the productivity of regional fisheries (Matsuura, 1996), and occurs throughout the year (Belem et al., 2013). The instabilities of the BC, with its meanders sometimes invading the shelf area (Campos et al., 2000), and the enhanced vertical transport driven by wind stress curl over the midshelf also impact oceanographic variability in the area. The region off Cabo Frio consequently represents a special oceanographic system that combines classical coastal Ekman upwelling and the typical oligotrophic western boundary current environment (Belem et al., 2013).

3. Material and methods

3.1. Sediment sampling and geochronology

A 245 cm long gravity-core (CF02–02B) was collected by the PSV Astro Garoupa (Petrobras support vessel) in 2002 from the Cabo Frio shelf (23°15′59″S, 41°48′01″W) at a water depth of 124 m (Fig. 1). The core was stored at 4 °C until it was open, described for its main sedimentological characteristics and sampled at intervals of 1 cm. A total of fourteen samples were selected for AMS ^{14}C-dating using either bulk organic matter or biogenic carbonate (Table 1). Analyses were performed by Beta Analytic in Florida, by the Arizona Radiochronology Laboratory in Tucson, Arizona, and also in Saclay, France. The AMS radiocarbon ages, corrected for their ^{13}C contents, were converted into calibrated radiocarbon ages using the Marine13 calibration curve (Reimer et al., 2013), a regional reservoir effect of $\Delta R = 8 \pm 17$ (Angulo et al., 2005), and considering the interval-error of 1σ using Calib 7.0 software (Stuiver and Reimer, 1993). Calibrated ages were interpolated from a smoothed cubic spline function using CLAM software (Blaauw, 2010) (Fig. 2).

Three AMS^{14}C dates (bulk organic carbon) were not considered for the elaboration of the age model. These dates were consistently younger than the general age-depth trend of the other eleven samples (Fig. 2). The deviations to younger ages of the discarded dates may reflect the effects of regional bioturbation, which is an important process in the water–sediment interface due to high oxygen availability in the bottom waters (Diaz et al., 2012; Sanders et al., 2014). Similar age inversions and inconsistencies between carbonate-based and

Table 1
Down-core conventional radiocarbon age, laboratory code, type of dated material and calibrated ages with their respective core-sample intervals.

Depth (cm)	Conventional radiocarbon age (yr B.P.)	Laboratory code	Material	Minimum 1σ	Calibrated radiocarbon age (yr B.P.)	Maximum 1σ
31	2615 ± 33	AA58021Pa413	Organic matter	1306	1822	2018
44	2835 ± 33	AA58022Pa414	Organic matter	2183	2532	2775
59	3480 ± 60	SacA00853	Organic matter	3165	3383	3707
70	2900 ± 50	*SacA003217	Organic matter	3874	4054	4431
90	5610 ± 90	SacA003218	Organic matter	5161	5393	5821
101	5455 ± 38	AA58023Pa415	Organic matter	5880	6162	6615
132	7530 ± 90	SacA00854	Organic matter	7851	8308	8851
143	9735 ± 45	SacA004833	Bryozoan	8512	9013	9589
159	8425 ± 44	*AA58024Pa416	Organic matter	9402	9941	10577
184	10830 ± 50	SacA003169	Bryozoan	10570	11218	12003
196	11240 ± 50	SacA003170	Bryozoan	11000	11750	12596
202	8160 ± 40	*Beta179276	Organic matter	11187	12005	12900
216	13010 ± 45	SacA003171	Bryozoan	11617	12590	13507
242	11350 ± 70	SacA003172	Bryozoan	12452	13524	14641

* Omitted from age model (see Section 3.1).

organic matter-based radiocarbon ages have also been observed in a core of coastal sediments from the Santos Basin (Mahiques et al., 2011). The age model was constructed from the remaining six bulk organic carbon and five biogenic carbonate AMS radiocarbon ages (Table 1).

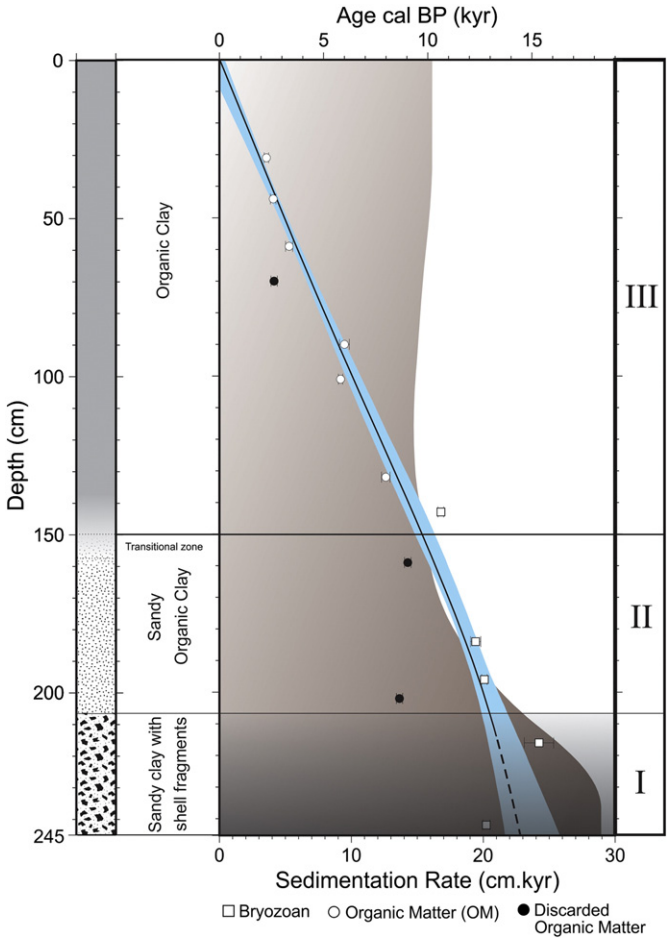

Fig. 2. The sediment column and the age-depth relation for Cabo Frio Core CF02–02B showing lithologic Units I, II and III. The eleven ^{14}C AMS dates employed to construct the age-depth curve are indicated as open symbols, whereas the three rejected dates that appear to reflect sediment disturbance are shown as solid symbols. Sedimentation rates are based on calibrated years that were calculated from Blaauw (2010).

3.2. Bulk sediment properties and geochemical analysis

X-ray diffraction (XRD) analyses were performed to identify the bulk and clay fraction (<2 μm) mineral assemblages. A total of 59 prewashed (deionized water and ethyl alcohol 60%) bulk sediment samples were air-dried, powdered and pressed in a powder holder. The clay fraction was decalcified using buffered 1 N sodium acetate ($CH_3COONa \cdot 3H_2O$). The insoluble fraction was disaggregated using ultrasound and subsequently wet-sieved (63 μm mesh). The fraction <63 μm was treated with heated (50 °C) H_2O_2 30% in order to eliminate organic matter and then centrifuged in order to separate the fraction <2 μm (clay fraction). An aliquot of the fraction was K-saturated (KCl) and then Mg-saturated ($MgCl_2$). Oriented mounts were prepared on glass slides and XRD scanned three times after being air-dried, glycolated and heated 550 °C/2 h (H) (Brown, 1972; Thorez, 1976) using a PANalytical X'PERT PRO MPD (PW 3040/60) equipped with a PW3050/60 goniometer (Theta/Theta) and Cu ($K\alpha_1$ = 1.54060 Å, 40 kV, 40 mA). Bulk samples were scanned from 3° to 70° two-theta in steps of 0.6° two-theta per minute, whereas clay fractions were scanned from 3° to 35° two-theta in steps of 0.02° two-theta per minute.

The main minerals identified through XRD were quantified by Fourier transform infrared spectrometry (FTIR) using a Perkin Elmer Spectrum 1000. For the FTIR analyses, the samples were ground to 2 μm to ensure validity of the Lambert–Beer Law and placed in a KBr pellet.

The mineral contents of the samples were quantified after measuring the individual spectra of the anticipated mineral components, making various blends of these components, measuring their spectra, and performing a multispectral analysis of the blended spectra (Bertaux et al., 1998).

Elemental analyses were performed on 67 samples (20 mg) that were taken at regular 3-cm intervals in the upper half of the core and at wider spacing (5-cm and 10-cm) in the bottom half. We focused our elemental analysis on the contents of Al, Ca, Ba, Fe, Mo and U in order to assess the importance of several different processes, including continental detrital input (Al, Fe), marine productivity (Ca and Ba), and redox shifts (Mo and U). The bulk dried and powdered sediment was digested with HF, HNO_3 and $HClO_4$ to achieve complete removal of organic matter and full dissolution of silicates and carbonates while retaining the biogenic calcium with the dissolved mineral matter (Jarvis and Jarvis, 1985). After the digestion procedure, a suite of major (Al, Fe and Ca) and trace (Ba, Mo and U) elements was analyzed using a Varian Liberty 200 ICP-AES and a Varian Ultra-Mass ICP-MS at the Institute de Recherche pour le Developpement, France. The instrument was calibrated by running blank and standard solutions prior to each elemental analysis. Recalibration checks were performed at regular intervals. All chemicals used in the study were analytical grade. The precision and accuracy of the elemental analyses were tested

using two duplicates of certified marine sediment (MESS-3, Canada), as a reference. The analytical reproducibility was 2.7% for the elements, whereas analytical accuracy was better than 3.4% for all of the elements except U (8.9%). Table S1 shows the values obtained from these procedures.

In addition to the trace element analyses, the concentrations of total organic carbon (TOC) in 122 sediment subsamples from 2-cm intervals were measured with a PDZ Europa ANCA-GSL CHN analyzer after the removal of inorganic carbon with 1N HCl. TOC concentrations are reported on a whole-sediment basis. The results were expressed as concentration (%, $mg \cdot g^{-1}$ or $\mu g \cdot g^{-1}$), fluxes and accumulation rates ($mg \cdot cm^{-2} \cdot kyrs^{-1}$). Fluxes and accumulation rates were calculated based on sedimentation rates, dry bulk density ($g \cdot cm^{-3}$) and minerals, trace elements and organic carbon content, where dry bulk density were evaluated by gravimetric measurements on 1 cm^3 samples.

4. Results

4.1. Geochronology, lithology, and sedimentation rates

Core CF02-02B represents the last ~14.4 calendar years before present (kyr CAL BP) based on the ^{14}C dating results. The core was devoid of laminations, as well as structures indicative of disturbance due to bioturbation. Three lithologic units were identified (Fig. 2), implying that major changes occurred in the depositional environment as this sediment sequence accumulated. The lower unit (I: 245–216 cm) accumulated from 14.4 to 12.9 kyr CAL BP and records the deposition of a layer of loamy sand (4/1-5Y dark gray) containing biogenic carbonate debris (shell fragments) contributing 39 ± 17% of carbonate contents (calcite + aragonite). Unit II (215–159 cm, 12.9 to 9.9 kyr CAL BP) also consists of sandy silt (4/2-5Y dark gray) but with lower carbonate contents (27 ± 12%) and no notable shell debris. The sedimentation rates decrease upwards through lithologic unit I from a high of 27.4 cm kyr^{-1} in the base to an average of 18.7 cm kyr^{-1} in unit II. The upper unit of Core CF02-02B (III: 159–1 cm) accumulated from 9.9 kyr cal BP to the present and has a homogeneous organic clay texture (4/2-5Y olive gray). Although unit III shows no clear lithologic change, sedimentation rates slightly increase at 50 cm (3.1 kyr CAL BP) from 14.7 cm kyr^{-1} in the lower part of the unit to 16.1 cm kyr^{-1} in the upper layer (Fig. 2).

4.2. Bulk mineral and trace element compositions and fluxes

Although sample-to-sample variability is sometimes large in the bulk mineralogy, the three sedimentary units have clearly different average values (Fig. 3). Basal unit I has markedly low fluxes of kaolinite, illite, quartz, and biogenic silica but elevated fluxes of carbonate minerals (calcite plus aragonite) and albite (Na-feldspar). The intermediate unit (II) shows generally higher fluxes of clay minerals (kaolinite + illite), quartz, and biogenic silica, whereas carbonate minerals sharply decrease, dropping to less than 30% of the deeper unit, and the contribution of albite drops to zero. Unit III begins with a decrease in the fluxes of carbonate minerals, quartz, and amorphous silica. However, the trend exhibited by unit II in the fluxes of clay minerals (kaolinite and illite) continues, and the albite flux remains at zero most of time. Finally, the upper layer of unit III, after 4 kyr, is marked by the reappearance of albite as sporadic flux peaks (Fig. 3).

Similar to the bulk mineral records, TOC and elemental concentrations and fluxes show different average values in the three lithological units (Fig. 4). Except for the Ca concentration, the concentrations of Al, Fe, Ba, U, Mo and TOC are relatively low in unit I and show a general up-core increase in concentrations. TOC concentrations are relatively constant between units I and II, with average values of 0.70 ± 0.27% in the bottom and 0.63 ± 0.13% in the upper unit, respectively. Throughout unit II, concentrations of Al, Fe, and Ba show a slight overall trend of increasing upward, whereas Ca shows an opposite behavior. Mo concentrations are quite variable in the sediments of unit III, but show an overall up-core tendency to decreasing values. Similar sample-to-sample variability is not evident in the sediments that were deposited before 9.9 kyr CAL BP (units I and II), which also have low Mo concentrations, suggesting that this variability is likely to be reflective of natural processes that affected the concentration of this trace

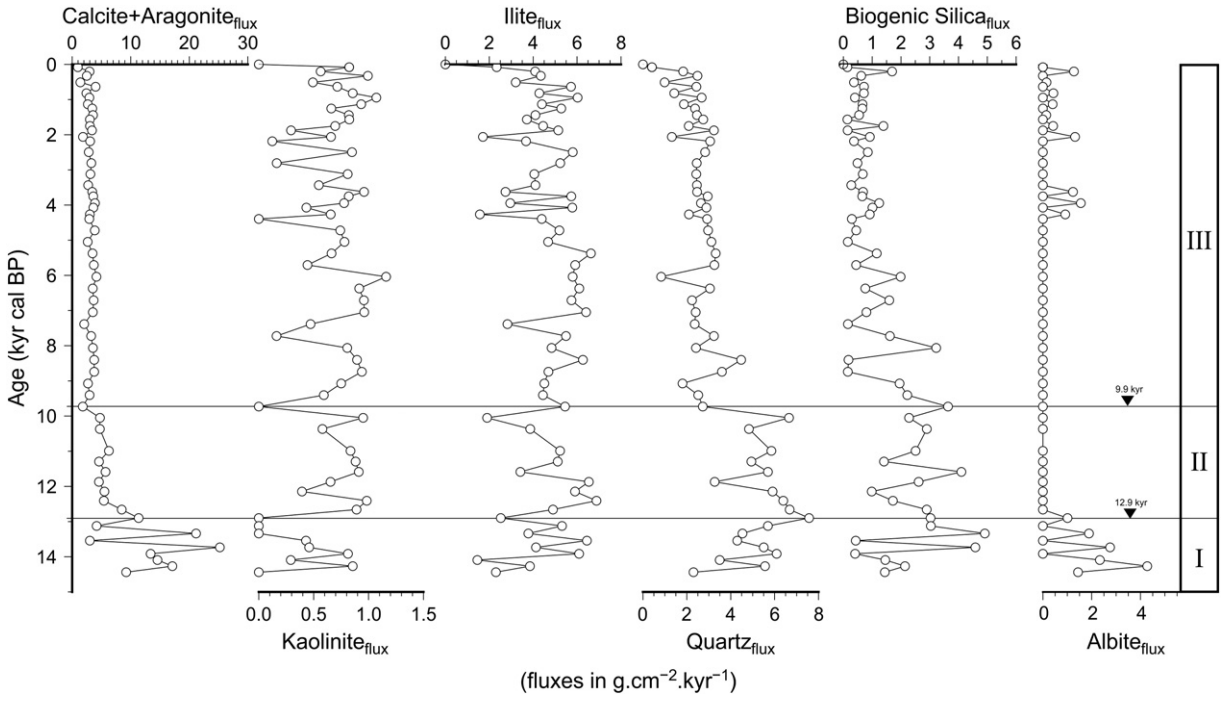

Fig. 3. Down-core profiles of the calcite + aragonite, kaolinite, illite, quartz, biogenic silica and albite fluxes ($g \cdot cm^{-2} \cdot kyr^{-1}$) in the sediments of Core CF02-02B in lithologic Units I, II and III.

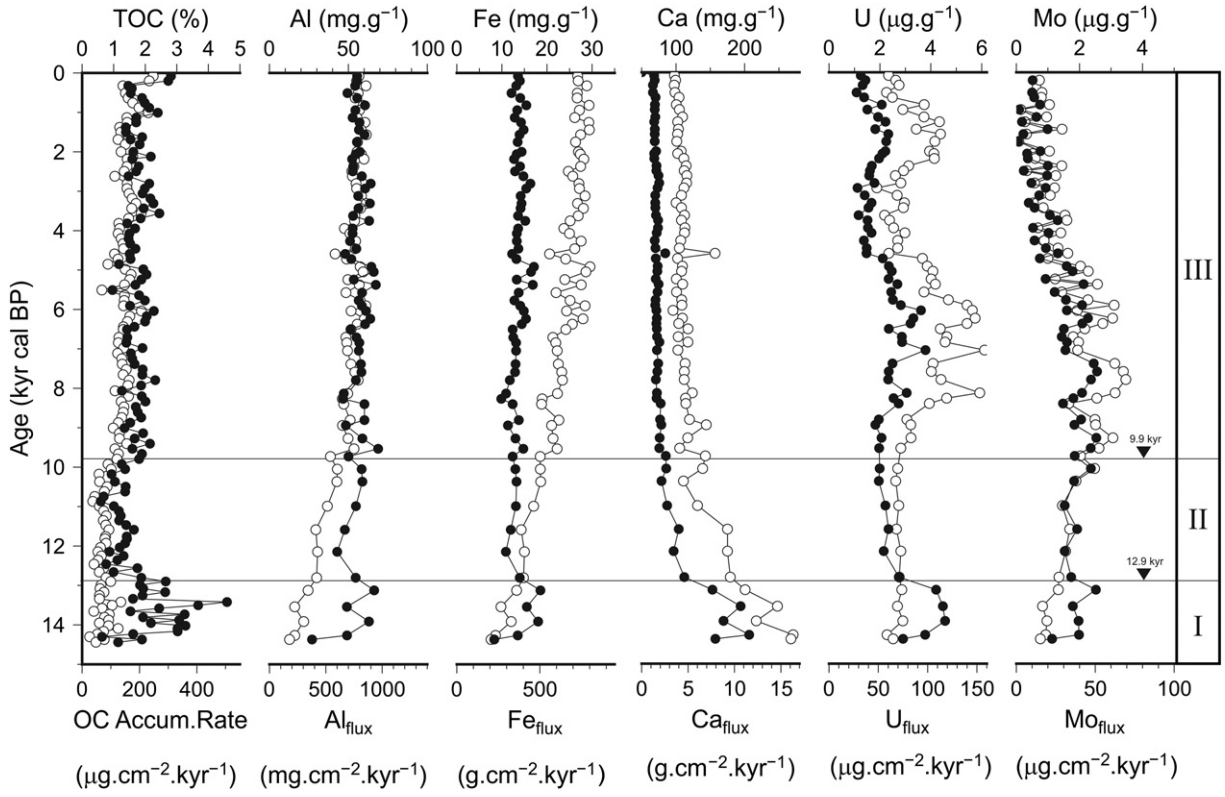

Fig. 4. Down-core profiles of the weight-weight concentrations (open circles) and fluxes (solid circles) of Total Organic Carbon (TOC), aluminum (Al), iron (Fe), calcium (Ca), uranium (U), and molybdenum (Mo) in the sediments of Core CF02–02B in lithologic Units I, II and III.

element and is not an artifact of its analysis. U concentrations were also very variable in unit III, showing a quite different pattern upward in the sediment sequence, peaking at the middle and upper of unit III (6 and 4.8 μg g^{-1}).

Elemental fluxes vary with changes in their individual concentrations, dry bulk density and bulk sedimentation rates. Unit I has slightly increasing upcore fluxes of Al, Fe, Ba and U, whereas unit II exhibits virtually constant values. Average TOC accumulation rates show an opposite trend that decreases from 120 ± 55.4 mgC cm^{-2} kyr^{-1} to 98 ± 31 mgC cm^{-2} kyr^{-1} between units I and II. The profiles of all six elements are very different in lithologic units I and II. Fluxes of TOC and Al, Fe, and Ba slightly increase in unit III (Fig. 4). However, the Ca flux remains practically unchanged after 9.9 kyr CAL BP, although it reaches its minimum in the top of the sequence, which is consistent with the lowest fluxes of carbonate minerals shown in Fig. 3. Like their concentrations, the fluxes of U and Mo are quite variable in unit III. Although the Mo flux decreases from unit II to unit III, the U flux peaks in the middle of unit III (Fig. 4).

5. Discussion

Variations in the mineral, elemental, and TOC concentrations and fluxes of the Core CF02-02B sediment sequence identify changes in the dynamics of sediment delivery and deposition on the Southeastern Brazilian Shelf since the late Pleistocene and throughout the Holocene. We first discuss the local impacts of postglacial sea level rise on sediment accumulation and bulk compositions, and then we assess the possible importance of *in situ* geochemical processes in affecting the trace element compositions. Finally, we consider the longer range influences of several paleoceanographic and paleoclimatic factors that are likely to have affected the delivery and accumulation of minerals and major and trace elements on the Cabo Frio continental shelf.

5.1. Effects of postglacial sea-level changes on the Cabo Frio continental shelf paleo-environments, sediment delivery, sediment accumulation, and paleoproductivity

Even though some details of the sea-level history on the Brazilian margin since the last glacial maximum remain to be better understood, it is recognized that the shelf has experienced three general phases of accelerated sea-level rise at respectively 11, 9 and 8 kyr BP (Kowsmann and Costa, 1979; Sawakuchi et al., 2009). These rises have undoubtedly affected the sediment lithology and the bulk mineral and elemental accumulation and composition of the Cabo Frio sediment record, which indeed indicates a succession of changes in the delivery and deposition of sediments over the past 14.4 kyr. These changes can be interpreted within the context of the paleoenvironmental and paleoceanographic factors that govern sediment accumulation and transport on continental shelves, including changes in water depth and turbulence, coastal erosion and deposition, and suspended loads of local rivers.

The three lithologic units in Core CF02-02B (Fig. 2) record the consequences of important changes in sedimentation processes on the continental shelf of Cabo Frio that are related to the major sea-level rises during the late Pleistocene and early Holocene, as schematically illustrated in Fig. 5. During the time period between 14.4 and 12.9 kyr CAL BP that corresponds to unit I, sedimentation in the area was under the strong influence of lowstand conditions (Angulo and Lessa, 1997; Kowsmann and Costa, 1979; Guilderson et al., 2000; Milne et al., 2005; Tarasov and Peltier, 2005) (Fig. 5B). The sandy texture and presence of carbonate debris from shell fragments in unit I (Fig. 2) indicate a high-energy nearshore depositional environment. Based on regional and global sea-level curves, the paleodepth at the core location was ~20 m at the beginning of this interval, or approximately 100 m below the current sea level, and the sandy texture of the sediments and the occurrence of broken shells indicate that the location was

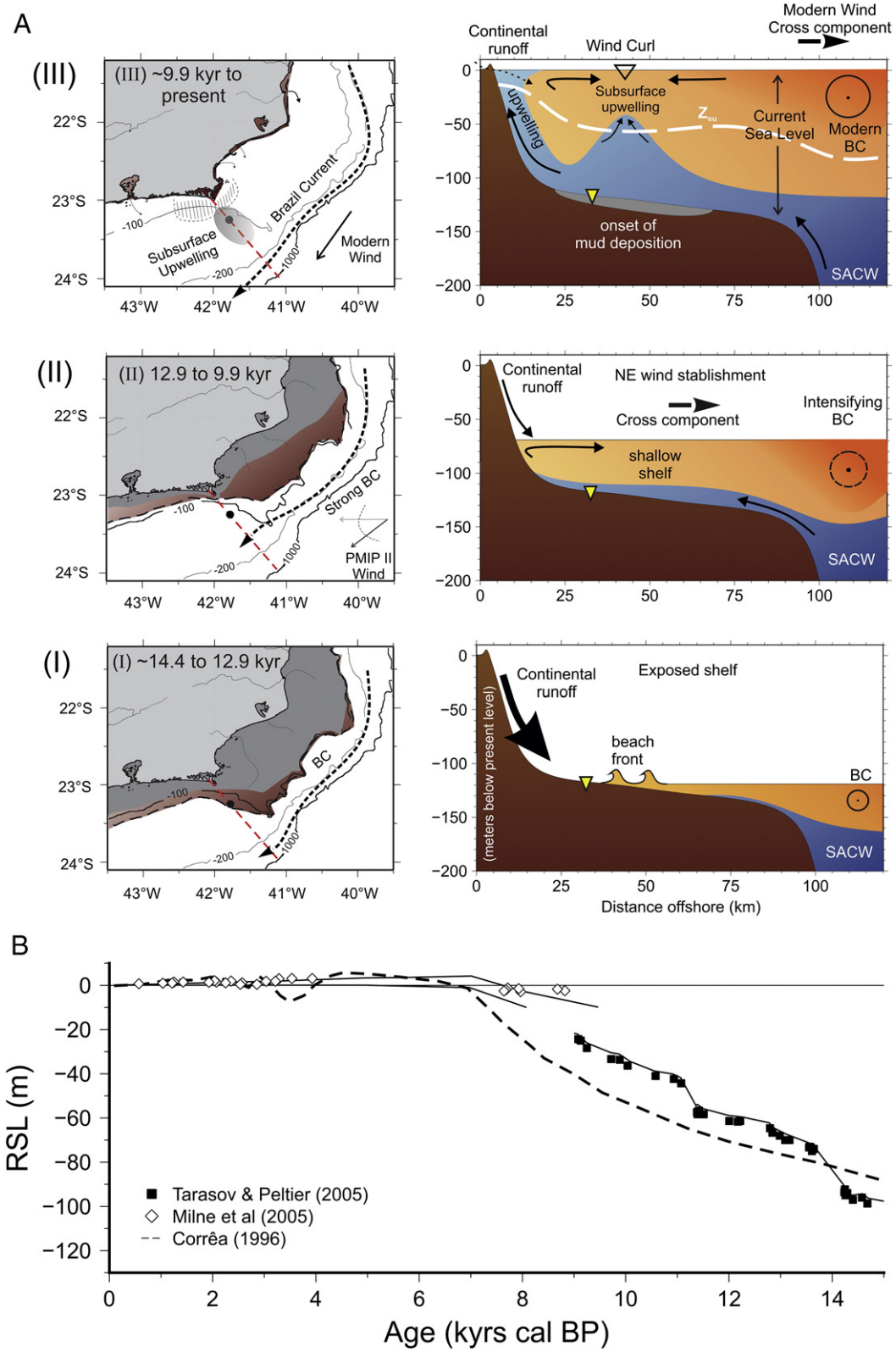

Fig. 5. A — Schematic depictions of the temporal evolution of Cabo Frio shelf over the last 14.4 CAL kyr BP (Lithologic Units I, II and III), showing the position and intensity of the Brazil Current (BC) and the South Atlantic Central Water (SACW). The dark gray area represents the progressive drowning of the coast as the shoreline retreated due to the sea-level rise. The intensity of continental runoff is marked by the thickness of arrows. The yellow triangle represents the location of Core CF02–02B. B — Sea-level changes over the last 15 kyr BP (Tarasov and Peltier, 2005; Milne et al., 2005; Angulo and Lessa, 1997; Guilderson et al., 2000).

subject to the strong coastal dynamics typical of a nearshore environment (Fig. 5). The presence of the shell debris is clear evidence for a shallow, nearshore setting in which surf turbulence prevented deposition of fine particles while permitting coarser particles to accumulate and to dilute the concentrations of TOC and trace elements (Fig. 4). Indeed, the coring site was close to the paleo-surf zone during

this interval as reconstructed by different sea-level curves (Fig. 5B) and also as interpreted by Kowsmann and Costa (1979) for the Cabo Frio region from the current 110 m contour line. This paleo-shoreline, now submerged 100 mbsl, may correspond to a 6-km-long NW–SE oriented linear rocky outcrop that rises about 2 m above the seafloor and that has been provisionally interpreted by Mendoza et al. (2014) as beach-rock. The presence of a beach-rock ridge indicates a stable period of lowered sea-level. Although no actual samples have yet been collected to confirm the beach-rock feature, previous studies have described this micro-relief as bioconstructional in origin (Reis et al., 2013; Mendoza et al., 2014). The reconstructed paleo-shoreline extends northeast into the Campos Basin and is defined by boundstone ridges that range from 4 to 10 m in height and that are formed of grainstones and contourites encrusted on top by red algae (Guistina, 2006).

The existence of a nearshore setting of the study site from 14.4 to 12.9 kyr CAL BP is supported by a number of factors. First, sediments deposited during this interval had relatively high accumulation rates (~22 $cm \cdot kyr^{-1}$, Fig. 2), high fluxes of carbonate biominerals, and increasing fluxes of quartz, biogenic silica, and clay minerals that suggest an increase in terrigenous material supply (Fig. 3), probably linked to closer proximity of the coring location to these mineral sources and river mouths owing to the lower sea level. Second, the high values of albite flux also point to the closer proximity of the sediment source to continent. Albite is a common primary-labile mineral produced by subaerial weathering of felsic igneous rocks; its presence reinforces the idea that the fluvial source of sediment delivery was nearer during this phase (Chou and Wollast, 1985; Knauss and Wolery, 1986) (Fig. 3). It is noteworthy that continental geological features of Rio de Janeiro's coastal area are characterized by the presence of a variety of Neoproterozoic and Paleozoic crystalline rocks with occasional Mesozoic dolerite intrusions, as typified by the exposures on Papagaios Island near Cabo Frio (Skrepnek et al., 2009). Another important source of feldspars to the sedimentation off Cabo Frio is the erosion of Barreiras formation that typically formed cliffs along the Brazilian coast north of Cabo Frio (see Supplementary material, Fig. S2) and whose erosion products were probably deposited during the existence of the now submerged coastal plain. Coastal erosion of these deposits was probably the main supply of albite to unit I.

The upper transitional zone of lithologic unit II (12.9 to 9.9 kyr CAL BP) corresponds to a time of progressive rapid sea-level rise (Fig. 5B). The sedimentation rate decreased during this stage from 22 $cm \cdot kyr^{-1}$ to ~18.7 $cm \cdot kyr^{-1}$, reflecting a more oceanic environmental setting with predominantly carbonate deposition. In terms of the global ocean, the estimated sea-level rise during the unit II time-frame was ca. 35 m (from ~−75 to −40 m). In the course of the sea-level rise, clay minerals, biogenic silica and quartz were deposited on the shelf, diluting the previously carbonate-dominated accumulation (Fig. 3). This change may well reflect a transition to a less turbulent depositional setting that allowed accumulation of finer sediments. The abrupt disappearance of the albite suggests that its weathering source was relatively more distant owing to the increase of sea level. The shoreline retreat and the expansion of the continental shelf during this phase modified the coastal oceanographic conditions (Fig. 5A), which may also be implied by the progressive decrease of biogenic Ca content (Fig. 4).

Three principal sources exist for the detrital sediments on the Cabo Frio shelf. The most important one is likely the Paraíba do Sul River that delivers continental sediments to the coastal ocean north of Cabo Frio, where they become entrained in the southward flowing nearshore current (Viana et al., 1998; Rodrigues-Filho et al., 2002; Guistina, 2006). This medium-sized river flows 1100 km through the Southeast Rift Basin north of the coastal mountains and crosses the states of São Paulo, Minas Gerais, and Rio de Janeiro before reaching the sea. Its catchment drains the mountains that surround the rift basin and also the north slopes of Rio de Janeiro State. A coastal lagoon south of Cabo São Tomé (Fig. 1) may mark the former mouth of the Paraíba do Sul River that consequently would have been closer to the core site location in the early Holocene. Indeed, a seaward excursion of the 80 m contour line south of Cabo São Tomé may trace the edge of the paleofan that was formed by this river when it was in its postulated former location. The river, therefore, could have more effectively delivered lithogenic material eroded from the crystalline rocks on adjacent continental areas to this portion of the shelf south of Cabo São Tomé in the late Pleistocene and early Holocene. A second possible sediment source is Guanabara Bay, which is located southwest of Cabo Frio (Fig. 1). Although this large bay now functions largely as a trap for sediments that are delivered by the several modest rivers that enter it, it was a river valley that reached the sea during times of lower sea level. Sufficient sediment has exited the bay and has been transported northeast by the longshore current to have smoothed the coastline and created the many lagoons that characterize this part of the coastline (Fig. 1). The northward transport of sediments exported by Guanabara Bay is clearly climate-induced, inasmuch as it is favored by equatorward cold-fronts that strengthen the coastal current. Finally, Albuquerque et al. (2014) showed through moored sediment trap collections on the Cabo Frio shelf break that the southward-flowing BC also transports some sediments that seem to have refractory properties to the Cabo Frio area.

The beginning of unit III, which was deposited after 9.9 ky CAL BP, marks the final stages of sea level rise and stabilization (Fig. 5B) and the positioning of the shoreline at a near-modern location (Fig. 5A) that eventually enabled the deposition of clay-size sediments in the offshore area (Kowsmann and Costa, 1979). A similar transition has been reported in the northern Santos Basin, where the depositional type changed between 8.8 to 8.3 kyr CAL BP from beach sands to sandy muds (Mahiques et al., 2011) and which supports the idea of regional sea level stabilization between 9 to 8 kyr CAL BP as proposed by Correa (1996).

After 9.9 kyr CAL BP, the changes in the trace element composition and in their individual fluxes, accompanied by the onset of the deposition of the homogeneous argillaceous sediment texture in unit III, most likely indicate the onset of deposition of the muddy bank formation in the mid-shelf area (Fig. 5a). The nature of this organic-carbon-rich (Fig. 4) and fine-grained sedimentary unit reflects deposition under a more productive surface setting and a deeper water column, and its timing corresponds well with the attainment of an essentially modern global sea level after the last glacial low stand (Milne et al., 2005; Tarasov and Peltier, 2005). These changes evidently also record the establishment of the upwelling system over the coring location. Prior to this time, the Cabo Frio upwelling system was unlikely to have developed over the coring site because the main flow of the BC would have been farther offshore from the coring site than in its present-day configuration (Fig. 5A).

The variations in the concentrations and fluxes of minerals (Fig. 3), metals, and organic carbon (Fig. 4) throughout the Holocene (unit III) were lower than those observed in previous units, indicating that sea-level changes seem to dominate control of the delivery of continental material for Cabo Frio shelf sediments. Furthermore, the variations in the concentrations and fluxes of U and Mo after 9.9 CAL kyr BP differed notably from those of the other elements (Fig. 4). The delivery of these redox-sensitive trace elements appears to have experienced sub-millennial variations. Downcore variations of U and Mo concentrations and fluxes were decoupled from the typical detrital elements, such as Al and Fe, suggesting control not only by changes in the delivery and provenance of these trace elements but also by variations in their authigenic deposition, which is modulated by redox-conditions at the water–sediment interface (Zheng et al., 2002; Tribovillard et al., 2012). According to Diaz et al. (2012), Cabo Frio shelf sediments present a highly dynamic redox setting. The deposition of abundant upwelling derived organic matter under an oxygenated water column produces a generally suboxic condition in the shelf sediments while favoring bioturbation that encourages organic matter oxidation. These complex and dynamic redox scenarios limit interpretation of the distributions of U

and Mo in Cabo Frio sediments, providing uncertainties in their use as paleoenvironmental proxies (Nameroff et al., 2002). However, we may hypothesize that U and Mo abundance fluctuations likely register the effects of primary production linked to coastal upwelling intensity that could contribute to the enrichment of these elements, superimposed on the effect of early diagenesis that can modify the original expression of the depositional environment. Thus, the enhancement of U concentrations and fluxes between 9 and 5 kyr CAL BP and again between 2.7 and 1 kyr CAL BP and the progressive upcore decrease in Mo may register changes in the organic matter-modulated diagenetic processes that are ultimately controlled by upwelling intensity. The fluxes of biogenic silica at the beginning of unit III, particularly between 9.9 and 6 kyr CAL BP, support the Holocene enhancement of marine productivity. This change was likely due to the reinforcement of coastal upwelling conditions and/or mid-shelf cold and nutrient-rich SACW intrusion into the euphotic zone (mid-shelf Ekman pumping) favored by wind stress curl over the mid-shelf [see Castelao and Barth (2006), Castelao (2012) for the modern configuration] (Fig. 5A). Intensifications of BC instability and their action over the shelf may have slowed the upwelling-driven offshore currents (Pereira and Castro, 2007), favoring the deposition of suspended loads on the mid-shelf. After 4 kyr CAL BP, the return of discrete peaks of albite associated with increasing fluxes of clay minerals indicates an enhancement of continental runoff input, possibly augmented by erosion of paleodeltas by wave action (Fig. 3). Modern conditions seem to have become established with the stabilization of sea level after 9 to 8 kyr CAL BP in the Cabo Frio Upwelling System (Fig. 5). Although Nagai et al. (2009), Gyllencreutz et al. (2010) have pointed to a tendency to recent strengthening of upwelling-induced primary productivity in the Cabo Frio region after 3 kyr CAL BP, the fluxes of metals, mineral, biogenic silica, and organic carbon accumulation reported here do not support this change.

5.2. Paleoclimate impacts on delivery of sediment to the Cabo Frio shelf

Climate-driven variations in the magnitude and locus of erosion in areas that are drained by rivers can lead to variations in the amounts and compositions of fluvial sediments that are delivered to the coastal ocean. Changes in rainfall are the primary agents in these variations over geologically short periods of time. Postglacial changes in erosion of the catchments of the Paraíba do Sul River and Guanabara Bay and in the oceanographic circulation modulated by climate govern the main mechanisms of sediment delivery, distribution, and deposition along the shelf and are likely to have influenced the differences in the mineral and elemental compositions of the three depositional units in Core CF02-02B. For example, the high rates of sedimentation of continental material on the Cabo Frio shelf at ~14 kyr CAL BP (Fig. 2), which we infer to be principally a depositional consequence of a lower sea level, may have been augmented by climate-induced increases in the delivery of land-derived sediment.

Precipitation in southeastern Brazil has a clear seasonal pattern in which most of the annual rainfall is associated with the summer presence of the South Atlantic Convergence Zone (SACZ), which is one of the main convective systems of South America and is an important feature of the SAMS (Zhou and Lau, 1998; Carvalho et al., 2004; Garreaud and Falvey, 2009). The SACZ is a feature formed by wind convergence and moisture advection that brings moisture from the Amazon region to central and southeastern Brazil (Carvalho et al., 2004). As in other monsoon systems, the SAMS is driven by land-sea thermal contrast. In addition, sea surface temperature of the South Atlantic Ocean can influence the intensity and position of the SACZ (Chaves and Nobre, 2004), which may modulate summer precipitation in southeastern Brazil. In contrast, winter precipitation is a mainly extratropical feature driven by increased frequency of cold front passages, which also enhance wave-driven littoral sediment remobilization (Alves and Pezzuto, 2009; Figueiredo et al., 2014).

The interval between 14.4 and 9.9 kyr CAL BP (units I and II) recorded in core CF02–02B represents a combined effect of low sea-level conditions and climate variability, complicating distinction of the effects of climate-induced processes in delivery material. It is worth restating that during the low stand maximum (−100 m) recorded in core CF02-02B, the core site was in a water depth of ca. 20 m, which prevents or at least strongly interferes with use of units I and II as archives for paleoclimatic reconstructions because of the water turbulence during their deposition.

After 9.9 kyr CAL BP, a depositional interval that includes the Holocene Hypsithermal, sea level changes were no longer the main factor controlling sediment delivery and deposition on the Cabo Frio shelf because the Holocene high stand had already nearly been achieved (Angulo and Lessa, 1997 — Fig. 5B). Instead, oceanographic changes linked to the NE wind-driven coastal upwelling intensity, the BC strength, and the action of mid-shelf wind curl stress were likely to be the main influences on shelf sediment deposition in this period. Some paleoclimate studies have shown that the mid-Holocene was marked by a dry climate in the Amazon Basin and in southeastern Brazil (Sifeddine et al., 2001; Nagai et al., 2009) that was likely associated with a weakening of the SAMS due to lower summer insolation (Silva Dias et al., 2009), but fluxes of clay minerals and the detrital elements Al and Fe were virtually constant throughout the entire Holocene (Figs. 3 and 4). The near-steady delivery of these detrital materials to the Cabo Frio shelf indicates little change in continental erosion and hence implies little climate change in their source areas since 9.9 kyr CAL BP. At the same time, the onset of organic-rich mud deposition off Cabo Frio during this interval represents evidence of an intensification of coastal upwelling and mid-shelf intrusions of SACW into the euphotic zone, marking the establishment of the modern oceanographic configuration of this western boundary upwelling system. The NE wind stress strengthening could lead to the establishment of a regional oceanographic circulation pattern in which the BC was potentially stronger, providing a strengthened and more proximal BC internal front action on the shelf processes, which would have increased productivity on the Cabo Frio shelf (Belem et al., 2013). This possibility is supported by the marked enhancements in fluxes of U and Mo (Fig. 4) and also by elevated values of the planktonic foraminifera ratio upwelling index (Lessa et al., 2014).

6. Summary and conclusions

We have studied the bulk mineral and major and trace element concentrations and fluxes of a core that provides a record of sedimentation on the Cabo Frio continental shelf of southeastern Brazil over the past 14.4 kyr CAL BP to assess the effects of sea-level changes, marine productivity, and climate changes on the delivery and deposition of the shelf sediments. The core was obtained from an oceanographically dynamic location in 124 m of water under the productive Cabo Frio upwelling system that is influenced by the interactions of the Brazil Current with several other water masses. Findings of our study can be summarized as:

- The global rise in sea level of ~100 m since 14.4 kyr CAL BP changed the depositional setting on the Cabo Frio shelf from a shallow-water, high-energy one to a deeper-water, lower-energy one. This change is most dramatically recorded in the sedimentary record at approximately 9 kyr CAL BP when deposition of earlier coarse-grained sediments containing biogenic carbonate debris was replaced by accumulation of muddy sediments rich in clay minerals.
- Despite their intimate relation to the high marine productivity associated with the Cabo Frio upwelling system, sediments at the coring site have accumulated in an oxic water column, but a suboxic seafloor setting that would favor deposition of redox-sensitive metals. Variations in fluxes of trace elements, including U and Mo, consequently provide evidence of changes in marine productivity.

- Postglacial and Holocene fluctuations in regional oceanographic circulation coupled with climate-induced changes in erosion of the catchments created shifts in trace element and mineral fluxes to the Cabo Frio shelf that allow reconstruction of paleoenvironmental histories.
- The modern upwelling system became positioned over the coring site after ~9 kyr CAL BP and appears to have experienced only small variations in its productivity intensity at this location since that time.

Supplementary data to this article can be found online at http://dx.doi.org/10.1016/j.palaeo.2016.01.006.

Acknowledgments

This study was funded by the Conselho Nacional de Desenvolvimento Científico e Tecnológico (CNPq) and the "Institut de Recherche pour le Développement (IRD France)" — LMI-PALEOTRACES, the Geochemistry Network of PETROBRAS/CENPES and the Brazilian National Petroleum and the Biofuels Agency (ANP) (Grant 0050.004388.08.9). Albuquerque is senior scholar from CNPq (Grant 306385/2013-9). We thank Prof. Joel Blum for his thoughtful comments on an earlier version of this contribution. We are also grateful to two anonymous reviewers for their helpful suggestions that helped us to further improve this paper.

References

Aguiar, A.L., Cirano, M., Pereira, J., Marta-Almeida, M., 2014. Upwelling processes along a western boundary current in the Abrolhos — Campos region of Brazil. Cont. Shelf Res. 85, 42–59.

Albuquerque, A.L.S., Belém, A., Zuluaga, F.J.B., Cordeiro, L.G.M., Mendoza, U., Knoppers, B.A., Gurgel, M.H.C., Meyers, P.A., Sifeddine, A., Capilla, R., 2014. Particle fluxes and bulk geochemical characterization of the Cabo Frio upwelling system in southeastern Brazil: sediment trap experiments between spring 2010 and summer 2012. An. Acad. Bras. Cienc. 84 (2), 601–619.

Alves, S., Pezzuto, P.R., 2009. Effect of cold fronts on the benthic macrofauna of exposed sandy beaches with contrasting morphodynamics. Braz. J. Oceanogr. 57 (2), 73–96.

Angulo, R.J., Lessa, G.C., 1997. The Brazilian sea-level curves: a critical review with emphasis on the curves from the Paranaguá and Cananéia regions. Mar. Geol. 140, 141–166.

Angulo, R.J., de Souza, M.C., Reimer, P., Sasaoka, S.K., 2005. Reservoir effect of the southern and southeastern Brazilian coast. Radiocarbon 47, 1–7.

Arz, H.W., Patzold, J., Wefer, G., 1998. Correlated millennial-scale changes in surface hydrography and terrigenous sediment yield inferred from last-glacial marine deposits off northeastern Brazil. Quat. Res. 50, 157–166.

Bard, E., Hamelin, B., Arnold, M., Montaggioni, L., Cabioch, G., Faure, G., Rougerie, F., 1996. Sea level record from Tahiti corals and the timing of deglacialmeltwater discharge. Nature 382, 241–244.

Barron, J.A., Bukry, D., 2007. Development of the California Current during the past 12,000 yr based on diatoms and silicoflagellates. Palaeogeogr. Palaeoclimatol. Palaeoecol. 248, 313–338.

Belem, A.L., Castelão, R.M., Albuquerque, A.L.S., 2013. Controls of subsurface temperature variability in a western boundary upwelling system. Geophys. Res. Lett. 40, 1362–1366.

Bertaux, J., Froehlich, P., IIdefonse, P., 1998. Multicomponent analysis of FTIR spectra: quantification of amorphous silica and crystallized mineral phases in synthetic and natural sediments. J. Sediment. Res. 68, 440–447.

Blaauw, M., 2010. Methods and code for "classical" age-modelling of radiocarbon sequences. Quat. Geochronol. 5, 512–518.

Bond, G., Showers, W., Cheseby, M., Lotti, R., Almasi, P., Menocal de, P., Priore, P., Cullen, H., Hajdas, I., Bonani, G., 1997. A pervasive millennial-scale cycle in North Atlantic Holocene and glacial climates. Science 278, 1257–1266.

Brown, G., 1972. The X-ray Identification and Crystal Structures Clay Minerals Mineralogical. Society Clay Mineral Groups, London (544p).

Brumsack, H.-J., 2006. The trace metal content of recent organic carbon-rich sediments: implications for Cretaceous black shale formation. Palaeogeogr. Palaeoclimatol. Palaeoecol. 232, 344–361.

Cainelli, C., Webster, U.M., 1999. General evolution of the eastern Brazilian continental margin. Lead. Edge 18, 800–805.

Calvert, S.E., Pedersen, T.F., 1993. Geochemistry of recent oxic and anoxic marine sediments: implications for the geological record. Mar. Geol. 113, 67–88.

Campos, E.J.D., Velhote, D., Silveira, I.C.A., 2000. Shelf break upwelling driven by Brazil Current cyclonic meanders. Geophys. Res. Lett. 27, 751–754.

Carvalho, E.E.V., Salomão, M.S.M.B., Molisani, M.M., Rezende, C.E., Lacerda, L.D., 2002. Contribution of a medium-sized tropical river to the particulate heavy metal load for the South Atlantic Ocean. Sci. Total Environ. 284, 85–93.

Carvalho, L.M.V., Jones, C., Liebmann, B., 2004. The South Atlantic Convergence Zone: persistence, intensity, form, extreme precipitation and relationships with intraseasonal activity. J. Clim. 17, 88–108.

Castelao, R.M., 2012. Seasurface temperature and wind stress curl variability near a cape. J. Phys. Oceanogr. 42, 2073–2087.

Castelao, R.M., Barth, J.A., 2006. The relative importance of wind strength and along-shelf bathymetric variations on the separation of a coastal upwelling jet. J. Phys. Oceanogr. 36, 412–425.

Castro, B.M.D., Miranda, L.B.D., 1998. Physical oceanography of the western continental shelf located between 4 N and 34 S. In: Robinson, A.R., Brink, K.H. (Eds.), The Sea. John Wiley & Sons, New York, pp. 209–251.

Chaves, R.R., Nobre, P., 2004. Interactions between sea surface temperature over the South Atlantic Ocean and the South Atlantic Convergence Zone. Geophys. Res. Lett. 31. http://dx.doi.org/10.1029/2003GL018647 (1–4 pp).

Chou, L., Wollast, R., 1985. Steady-state kinetics and dissolution mechanism of albite. Am. J. Sci. 285, 963–993.

Correa, I.C.S., 1996. Les variations du niveau de la merdurant les derniers 17.500 ans BP: l'exemple de la plateformecontinentale du Rio Grande do Sul – Brésil. Mar. Geol. 130, 163–178.

Crusius, J., Calvert, S., Pedersen, T., Sage, D., 1996. Rhenium and molybdenum enrichments in sediments as indicators of oxic, suboxic and sulfidic conditions of deposition. Earth Planet. Sci. Lett. 145, 65–78.

Diaz, R., Moreira, M., Mendoza, U., Machado, W., Böttcher, M.E., Santos, H., Belem, A.L., Capilla, R., Esscher, P., Albuquerque, A.L., 2012. Early diagenesis of sulfur in a tropical upwelling system, Cabo Frio, southeastern Brazil. Geology 40 (10), 879–882.

Diester-Haass, L., Meyers, P.A., Vidal, L., 2002. The late Miocene onset of high productivity in the Benguela Current upwelling system as part of a global pattern. Mar. Geol. 180, 87–103.

Dymond, J., Suess, E., Lyle, M., 1992. Barium in deep-sea sediments: a proxy for paleoproductivity. Paleoceanography 7, 163–181.

Fainstein, R., Summerhayes, C.P., 1982. Structure and origin of marginal banks off Eastern Brazil. Mar. Geol. 46, 199–215.

Figueiredo Jr., A.G., de Toledo, M.B., Cordeiro, R.C., Godoy, J.M.O., da Silva, F.T., Vasconcelos, S.C., dos Santos, R.A., 2014. Linked variations in sediment accumulation rates and sea-level in Guanabara Bay, Brazil, over the last 6000 years. Palaeogeogr. Palaeoclimatol. Palaeoecol. 415, 83–90.

Franchito, S.H., Oda, T.O., Brahmananda, R.V., Kayano, M.T., 2008. Interaction between coastal upwelling and local winds at Cabo Frio, Brazil: an observational study. J. Appl. Meteorol. Climatol. 47, 1590–1598.

François, R., Honjo, S., Manganini, S.J., Ravizza, G.E., 1995. Biogenic barium fluxes to the deep sea: implications for paleoproductivity reconstruction. Glob. Biogeochem. Cycles 9, 289–303.

Garreaud, R., Falvey, M., 2009. The coastal winds off western subtropical South America in future climate scenarios. Int. J. Climatol. 29, 543–554.

Guilderson, T.P., Burckle, L., Hemming, S., Peltier, W.R., 2000. Late Pleistocene sea level variations derived from the Argentine shelf. Geochem. Geophys. Geosyst. 1. http://dx.doi.org/10.1029/2000GC000098.

Guistina, I.D.D., 2006. Sedimentação carbonática de algas vermelhas coralináceas da plataforma continental da Bacia de Campos: um modelo carbonático análogo para o terciário PhD Thesis Universidade Federal do Rio Grande do Sul, p. 120.

Gyllencreutz, R., Mahiques, M.M., Alves, D.V.P., Wainer, I.K.C., 2010. Mid- to late-Holocene paleoceanographic changes on the southeastern Brazilian shelf based on grain size records. The Holocene 20, 863–875.

Hemming, S.R., 2004. Heinrich events: massive late Pleistocene detritus layers of the North Atlantic and their global imprint. Rev. Geophys. 42 (RG 1005).

Jarvis, I.J., Jarvis, K., 1985. Rare earth element geochemistry of standard sediments: a study using inductively coupled plasma spectrometry. Chem. Geol. 53, 335–344.

Jennerjahn, T., Knoppers, A.B., de Sousa, W., Carvalho, C., Mollanhaue, G., Hubner, M., Ittekkot, V., 2010. The Tropical Brazilian Continental Margin. In: Liu, K., et al. (Eds.), Carbon and Nutrient Fluxes in Continental Margins, a Global Synthesis. Springer Verlag Heidelberg, Berlin, pp. 427–436.

Keil, R.G., Hedges, J.I., 1993. Sorption of organic matter to mineral surfaces and the preservation of organic material in coastal marine sediments. Chem. Geol. 107, 385–388.

Knauss, I.G., Wolery, T.J., 1986. Dependence of albite dissolution kinetics on pH and time at 25 f and 70 'C. Geochim. Cosmochim. Acta 50, 2481–2497.

Kowsmann, R.O., Costa, M.P.A., 1979. Sedimentação Quaternária da margem continental brasileira e das áreas oceânicas adjacentes. Projeto REMAC — Reconhecimento Global da margem continental brasileira. PETROBRAS/CENPES/DINTEP/CPRM/DHN/CNPq, Rio de Janeiro, Brasil, pp. 9–55.

Leduc, G., Vidal, L., Tachikawa, K., Rostek, F., Sonzogni, C., Beaufort, L., Bard, E., 2007. Moisture transport across Central America as a positive feedback on abrupt climate changes. Nature 445, 908–911.

Lessa, D.V.O., Ramos, R.P., Barbosa, C.F., da Silva, A.R., Belem, A., Turcq, B., Albuquerque, A.L., 2014. Planktonic foraminifera in the sediment of a western boundary upwelling system off Cabo Frio, Brazil. Mar. Micropaleontol. 106, 55–68.

Mahiques, M.M., Silveira, I.C.A., Sousa, S.H.M., Rodrigues, M., 2002. Post-LGM sedimentation on the outer shelf–upper slope of the northernmost part of the São Paulo Bight, southeastern Brazil. Mar. Geol. 181, 387–400.

Mahiques, M.M., Tessler, M.G., Ciotti, A.M., Silveira, I.C., Sousa, S.H.M., Figueira, R.C.L., Tassinari, C.C.G., Furtado, V.V., Passos, R.F., 2004. Hydrodynamically driven patterns of recent sedimentation in the shelf and upper slope off Southeast Brazil. Cont. Shelf Res. 24, 1685–1697.

Mahiques, M., Sousa, S.H.M., Burone, L., Nagai, R.H., Silveira, I.C.A., Figueira, R.C.L., Soutelino, R.G., Ponsoni, L., Klein, D., 2011. Radiocarbon geochronology of the sediments of the São Paulo Bight (southern Brazilian upper margin). An. Acad. Bras. Cienc. 83, 817–834.

Matsuura, Y., 1996. A probable cause of recruitment failure of Brazilian Sardine (Sardinellaaurita) population during the 1974/75 spawning season. S. Afr. J. Mar. Sci. 17, 29–35.

Mendoza, U., Neto, A.A., Abuchacra, R.C., Barbosa, C.F., Figueiredo Jr., A.G., Gomes, M.C., Belem, A.L., Capilla, R., Albuquerque, A.L.S., 2014. Geoacoustic character, sedimentology and chronology of a cross-shelf Holocene sediment deposit off Cabo Frio, Brazil (southwest Atlantic Ocean). Geo-Mar. Lett. 34 (4), 297–314.
Meyers, P.A., 1997. Organic geochemical proxies of paleoceanographic, paleolimnologic, and paleoclimatic processes. Org. Geochem. 27 (5), 213–250.
Milne, G.A., Long, A.J., Bassett, S.E., 2005. Modelling Holocene relative sea-level observations from the Caribbean and South America. Quat. Sci. Rev. 24, 1183–1202.
Muscheler, R., Kromer, B., Björck, S., Svensson, A., Friedrich, M., Kaiser, K.F., Southon, J., 2008. Tree rings and ice cores reveal 14C calibration uncertainties during the Younger Dryas. Nat. Geosci. 1, 263–2687.
Nagai, R.H., Sousa, S.H.M., Burone, L., Mahiques, M.M., 2009. Paleoproductivity changes during the Holocene in the inner shelf of Cabo Frio, southeastern Brazilian continental margin: Benthic foraminifera and sedimentological proxies. Quat. Int. 206, 62–71.
Nameroff, T.J., Balistrieri, L.S., Murray, J.W., 2002. Suboxic trace metals geochemistry in the eastern tropical North Pacific. Geochim. Cosmochim. Acta 66 (7), 1139–1158.
Oliveira, D.R.P., Cordeiro, L.G.M.S., Carreira, R.S., 2013. Characterization of organic matter in cross-margin sediment transects of an upwelling region in the Campos Basin (SW Atlantic, Brazil) using lipids biomarkers. Biogeochemistry 112, 311–327.
Pereira, A.F., Castro, B.M., 2007. Internal tides in the southwestern Atlantic off Brazil: observations and numerical modeling. J. Phys. Oceanogr. 37, 1512–1526.
Peterson, R.G., Stramma, L., 1991. Upper-level circulation in the South Atlantic Ocean. Prog. Oceanogr. 26, 1–73.
Piola, A.R., Campos, E.J.D., Mö¨ller Jr., O.O., Charo, M., Martinez, C.M., 2000. Subtropical shelf front off eastern South America. J. Geophys. Res. 105, 6566–6578.
Pisias, N.G., Mix, A.C., Heusser, L., 2007. Millennial scale climate variability of the northeast Pacific Ocean and northwest North America based on radiolária and pollen. Quat. Sci. Rev. 20, 1561–1576.
Reimer, P.J., Bard, E., Bayliss, A., Beck, J.W., Blackwell, P.G., Ramsey, C.B., Buck, C.E., Cheng, H., Edwards, R.L., Friedrich, M., Grootes, P.M., Guilderson, T.P., Haflidason, H., Hajdas, J., Hatté, C., Heaton, T.J., Hoffmann, D.L., Hogg, A.G., Hughen, K.A., Kaiser, K.F., Kromer, B., Manning, S.W., Niu, M., Reimer, R.W., Richards, D.A., Scott, E.M., Southon, J.R., 2013. INTCAL13 and Marine13 radiocarbon age calibration curves 0–50,000 years cal BP. Radiocarbon 55 (4), 1869–1887.
Reis, A.T., Maia, R.M.C., Silva, C.G., Rabineau, M., Guerra, J.V., Corini, C., Ayres, A., Arantes-Oliveira, R., Benabdellouahed, M., Simões, I., Tardin, R., 2013. Origin of step-like and lobate seafloor features along the continental shelf off Rio de Janeiro State, Santos basin-Brazil. Geomorphology 203, 25–45.
Rodrigues-Filho, S., Behling, H., Irion, G., Müller, G., 2002. Evidence for lake formation in response to inferred Holocene climatic transition in Brazil. Quat. Res. 57, 131–137.
Roughan, M., Middleton, J.H., 2002. A comparison of observed upwelling mechanisms off the east coast of Australia. Cont. Shelf Res. 22, 2551–2572.
Sanders, C.J., Caldeira, P.P., Smoak, J.M., Ketterer, M.E., Belem, A., Mendoza, U.M.N., Cordeiro, L.G.M.S., Silva-Filho, E.V., Patchineelam, S.R., Albuquerque, A.L.S., 2014. Recent organic carbon accumulation (100 years) along the Cabo Frio, Brazil upwelling region. Cont. Shelf Res. 75, 68–75.
Sawakuchi, A.O., Giannini, P.C.F., Martinho, C.T., Tanaka, A.P.B., 2009. Grain-size and heavy minerals of the Late Quaternary eolian sediments from the Imbituba–Jaguaruna coast, Southern Brazil: depositional controls linked to relative sea-level changes. Sediment. Geol. 222, 226–240.
Silveira, I.C.A., Schmidt, A.C.K., Campos, E.J., de Godoi, S.S., Ikeda, Y., 2000. A Corrente do Brasil ao largo da costa leste brasileira. Rev. Bras. Oceanogr. 48, 171–183.
Sifeddine, A., Martin, L., Turcq, B., Volkemer-Ribeiro, C., Soubiès, F., Cordeiro, R.C., Suguio, K., 2001. Variations of Amazonian Rain Forest environments: a sedimetological records covering 30,000 years BP. Palaeogeogr. Palaeoclimatol. Palaeoecol. 168, 221–235.
Silva Dias, P.L., Turcq, B., Silva Dias, M.A.F., Braconnot, P., Jorgetti, T., 2009. Evaluation of a model simulation of 6 ka BP and present climate in tropical South America. In: Vimuex, F., et al. (Eds.), Past Climate Variability from the last Last Glacial Maximum to the Holocene in South American and Surrounding RegionsDevelopments in Paleoenvironmental Research Series (DPER) vol. 14. Springer Verlag, pp. 259–281 (12 pp).
Skrepnek, C.C., Schmitt, R.S., Guerra, J.V., 2009. Geology and geomorphology of Papagaios Island, Cabo Frio, SE Brazil. J. Coast. Res. 56, 767–771.
Souto, D.D., Lesa, D.O., Albuquerque, A.S., Sifeddine, A., Turcq, B.J., Barbosa, C.F., 2011. Marine sediments from southeastern Brazilian continental shelf: a 1200 year record of upwelling productivity. Palaeogeogr. Palaeoclimatol. Palaeoecol. 299, 49–55.
Stríkis, N.M., Cruz, F.W., Cheng, H., Karmann, I., Edwards, R.L., Vuille, M., Wang, X., de Paula, M.S., Novello, V.F., Auler, A.S., 2011. Abrupt variations in South American monsoon rainfall during the Holocene based on a speleothem record from central-eastern Brazil. Geology 1075–1078.
Stuiver, M., Reimer, P.J., 1993. Extended 14C data base and revised CALIB 3.0 '4C age calibration program. In: Stuiver, M., Long, A., Kra, R.S. (Eds.), Calibration 1993. Radiocarbon 35, pp. 215–230.
Swarzenski, P.W., Baskaran, M., Rosenbauer, R.J., Orem, W.H., 2006. Historical trace element distribution in sediments from the Mississippi River delta. Estuar. Coasts 29, 1094–1107.
Tarasov, L., Peltier, W.R., 2005. Arctic freshwater forcing of the Younger Dryas cold reversal. Nature 435, 662–665.
Thorez, J., 1976. Pratical Identification of Clay Minerals. G. Lelote, Belgic (90p).
Treguer, P., Nelson, D.M., van Bennekom, A.J., de Master, D.J., Leynaert, A., Queguiner, B., 1995. The silica balance in the world ocean: a reestimate. Science 268, 375–379.
Tribovillard, N., Algeo, T.J., Lyons, T., Riboulleau, A., 2006. Trace metals as paleoredox and paleoproductivity proxies: an update. Chem. Geol. 232, 12–32.
Tribovillard, N., Algeo, T.J., Bandin, F., Riboulleau, A., 2012. Analysis of marine environmental conditions based on molybdenum-uranium covariation — application to Mesozoic paleoceanography. Chem. Geol. 324-325, 46–58.
Venancio, I.M., Belem, A.L., Santos, T.H.R., Zucchi, M.R., Azevedo, A.E.G., Capilla, R., Albuquerque, A.L.S., 2014. Influence of continental shelf processes in the water mass balance and productivity from stable isotope data on the Southeastern Brazilian coast. J. Mar. Syst. 139, 241–247.
Viana, A.R., Faugères, J.C., Kowsmann, R.O., Lima, J.A., Caddah, L.E.G., Rizzo, J.G., 1998. Hydrology, morphology and sedimentology of the Campos continental margin, offshore Brazil. Sediment. Geol. 115, 133–157.
Vuille, M., Burns, S.J., Taylor, B.L., Cruz, F.W., Bird, B.W., Abbott, M.B., Kanner, L.C., Cheng, H., Novello, V.F., 2012. A review of the South American monsoon history as recorded in stable isotopic proxies over the past two millennia. Clim. Past 8, 1309–1321.
Warning, B., Brumsack, H.-J., 2000. Trace metal signatures of eastern Mediterranean sapropels. Palaeogeogr. Palaeoclimatol. Palaeoecol. 190, 165–194.
Yoshinaga, M.Y., Sumida, P.Y.G., Wakeham, S.G., 2008. Lipid biomarkers in surface sediments from an unusual coastal upwelling area from the SW Atlantic Ocean. Org. Geochem. 39, 1385–1399.
Zheng, Y., Anderson, R.F., van Geen, A., Fleisher, M.Q., 2002. Preservation of particulate non-lithogenic uranium in marine sediments. Geochim. Cosmochim. Acta 66 (17), 3085–3092.
Zhou, J., Lau, K.-M., 1998. Does a monsoon climate exist over South America? J. Clim. 11, 1020–1040.